

Electronic Supplementary Information

N, S dual doping strategy via electrospinning to prepare hierarchically porous carbon polyhedra embedded carbon nanofibers for flexible supercapacitors

Yanjiang Li^a, Guang Zhu^b, Hailong Huang^{a*}, Min Xu^a, Ting Lu^a and Likun Pan^{a*}

^aShanghai Key Laboratory of Magnetic Resonance, School of Physics and Materials Science, East

China Normal University, Shanghai 200062, P. R. China

^bKey Laboratory of Spin Electron and Nanomaterials of Anhui Higher Education Institutes, Suzhou Un

iversity, Suzhou 234000, P. R. China

* Corresponding author. Tel: +86 21 62234132; Fax: +86 21 62234321. E-mail:

lkpan@phy.ecnu.edu.cn (Likun Pan); huanghao3310774@163.com (Hailong Huang)

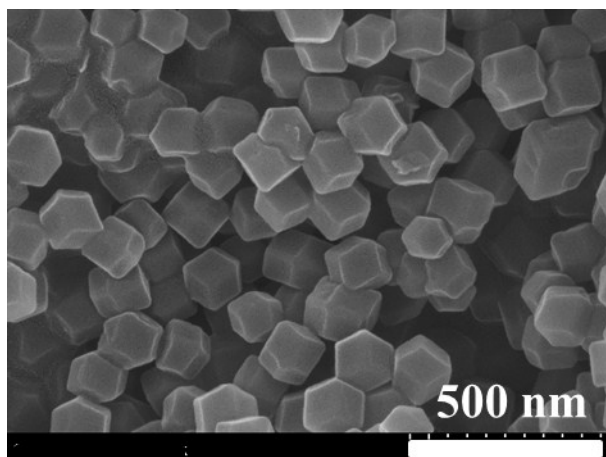


Fig. S1 FESEM image of ZIF-67.

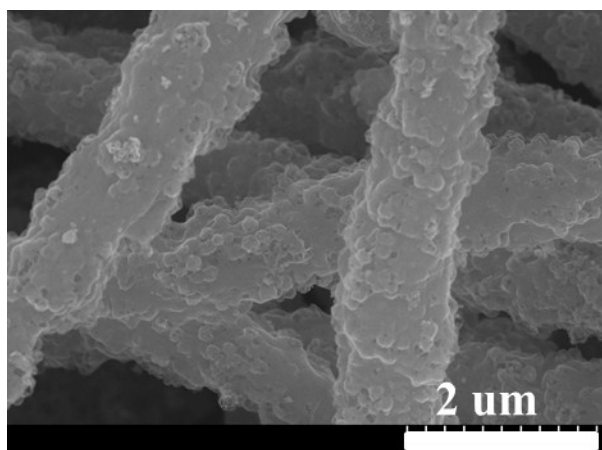


Fig. S2 FESEM image of CPCNF precursor after electrospinning.

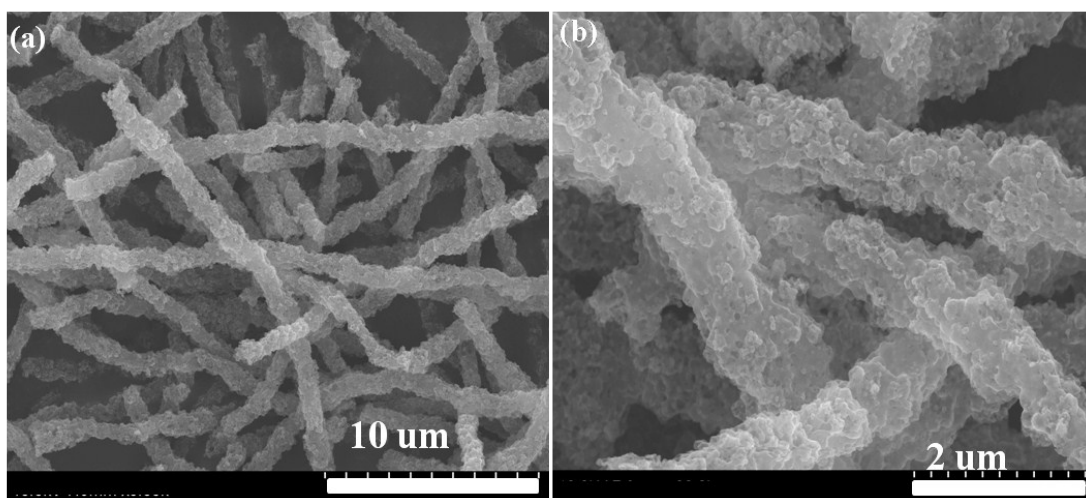


Fig. S3 FESEM images of Co-CPCNF at (a) low- and (b) high-magnification.

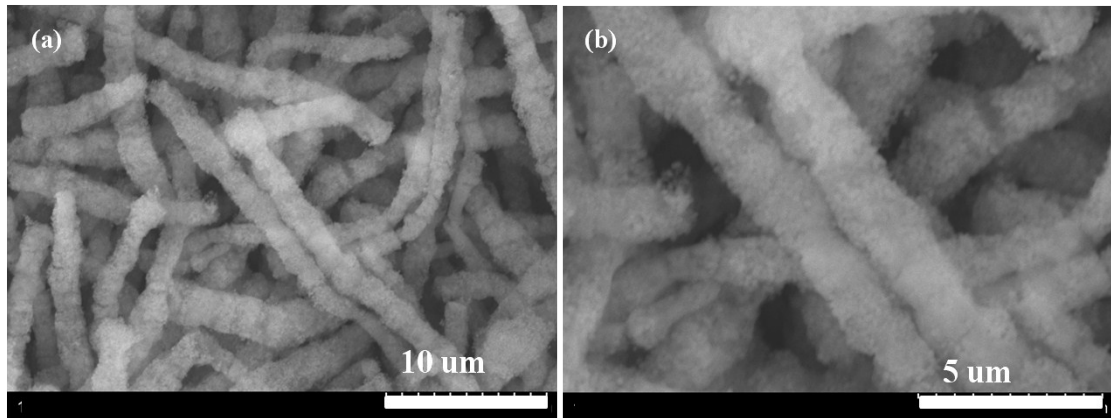


Fig. S4 FESEM images of NSCPCNF precursor after electrospinning at (a) low- and (b) high-magnification.

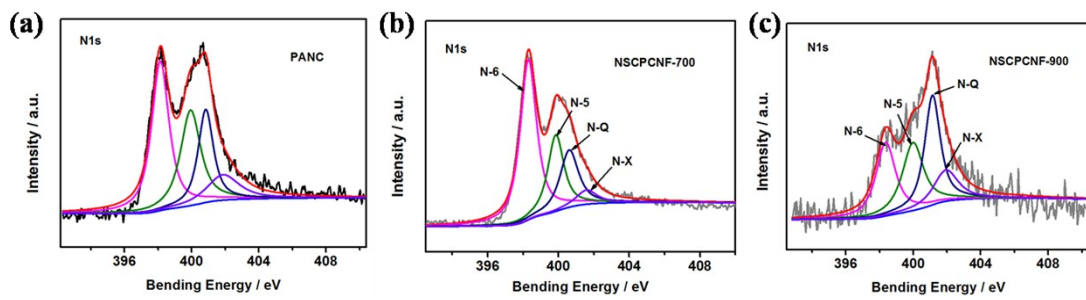


Fig. S5 High resolution N1s spectra of PANC (a), NSCPCNF-700 (b) and NSCPCNF-900 (c).

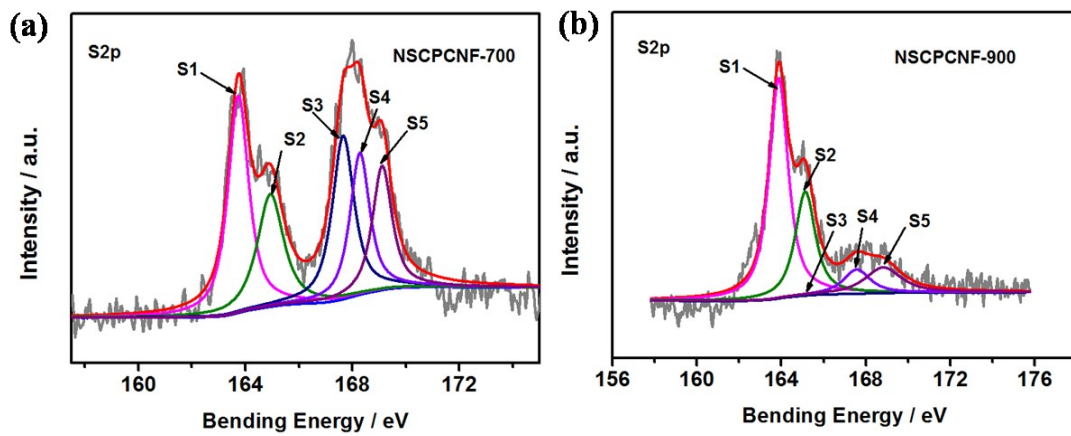


Fig. S6 High resolution S2p spectra of NSCPCNF-700 (a) and NSCPCNF-900 (b).

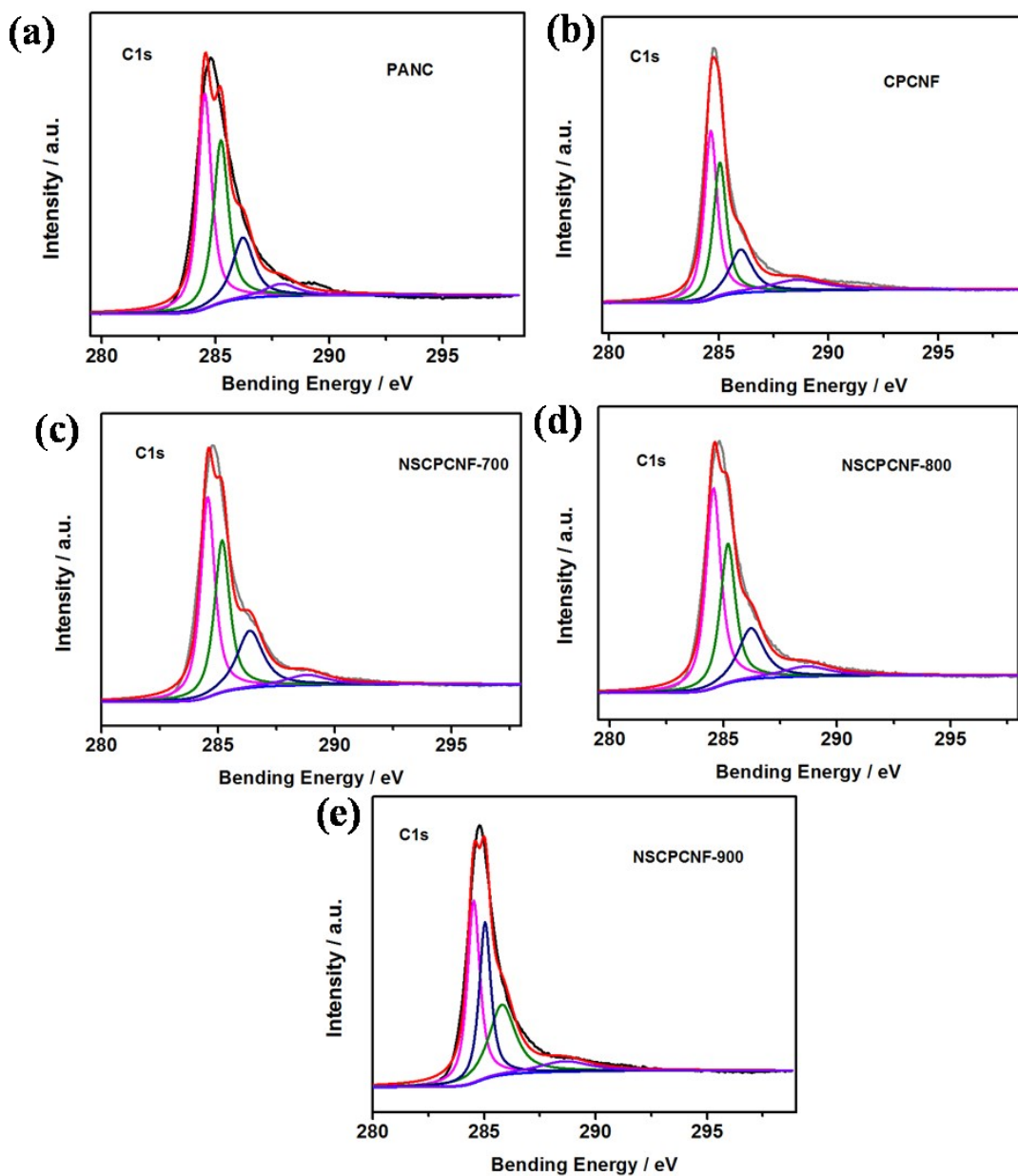


Fig. S7 High resolution C1s spectra of PANC (a), CPCNF (b), NSCPCNF-700 (c), NSCPCNF-800 (d),

NSCPCNF-900 (e).

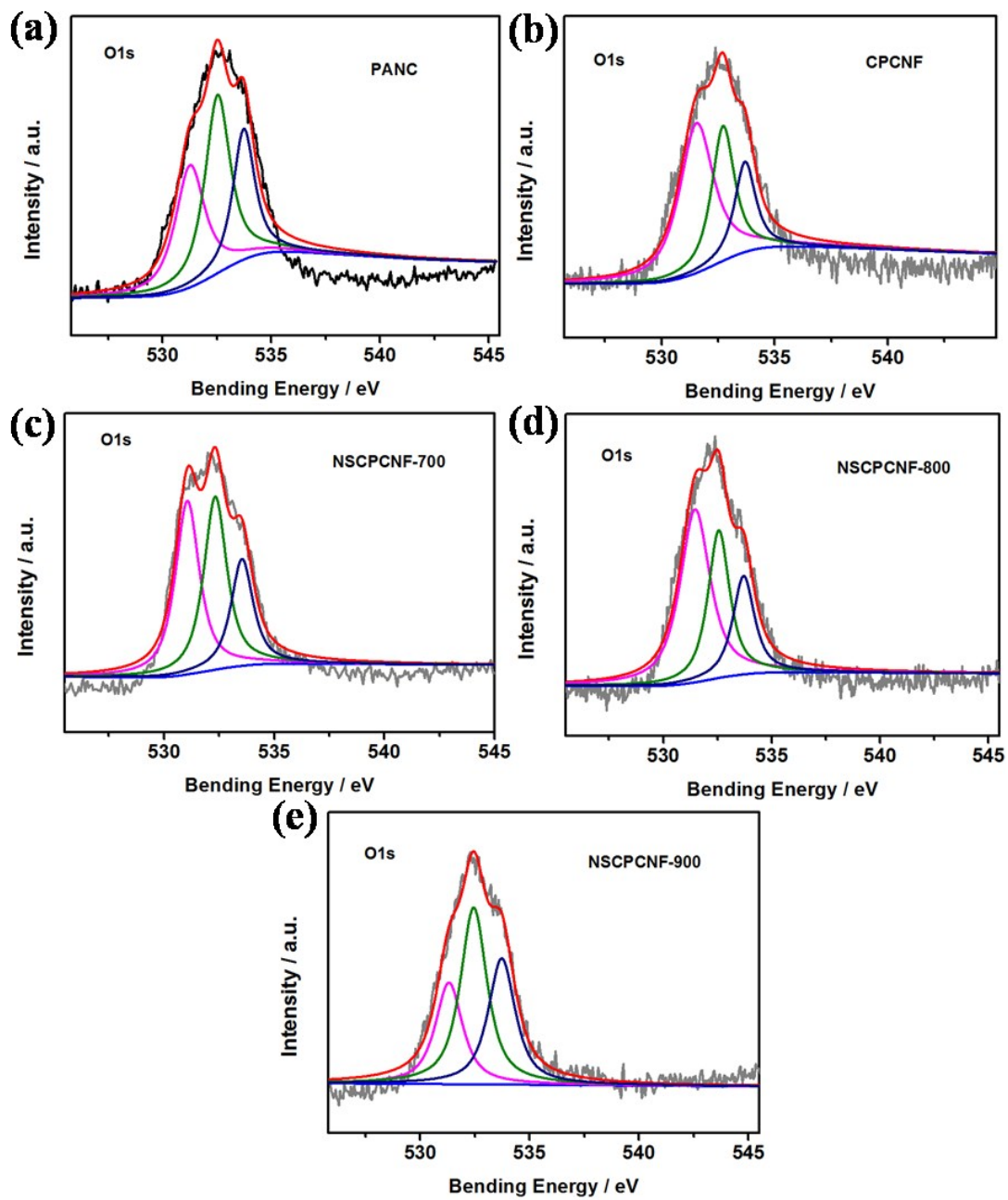


Fig. S8 High resolution O1s spectra of PANC (a), CPCNF (b), NSCPCNF-700 (c), NSCPCNF-800 (d),

NSCPCNF-900 (e).

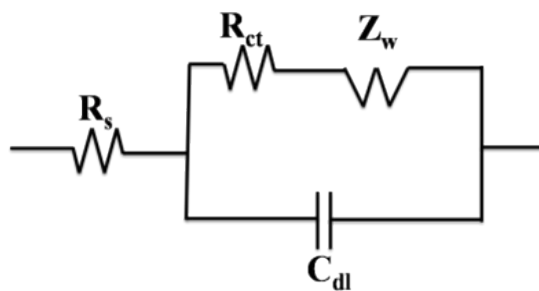


Fig. S9 Equivalent circuit model for Nyquist plots of PANC, CPCNF and NSPCNF.

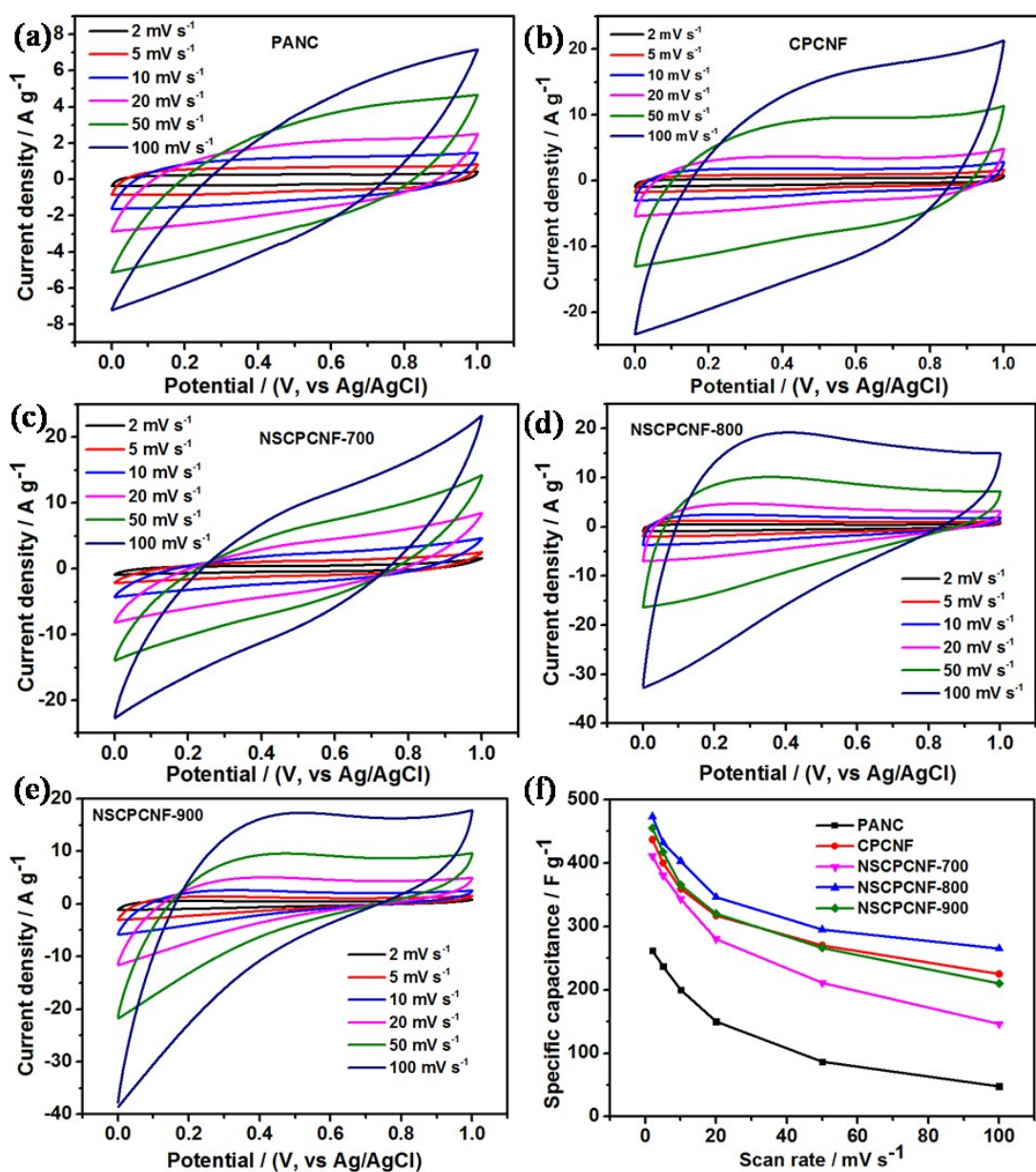


Fig. S10 CV curves of PANC (a), CPCNF (b), NSPCNF-700 (c), NSPCNF-800 (d), NSPCNF-900 (e).

Specific capacitances of PANC, CPCNF and NSCPCNF at different scan rates (f).

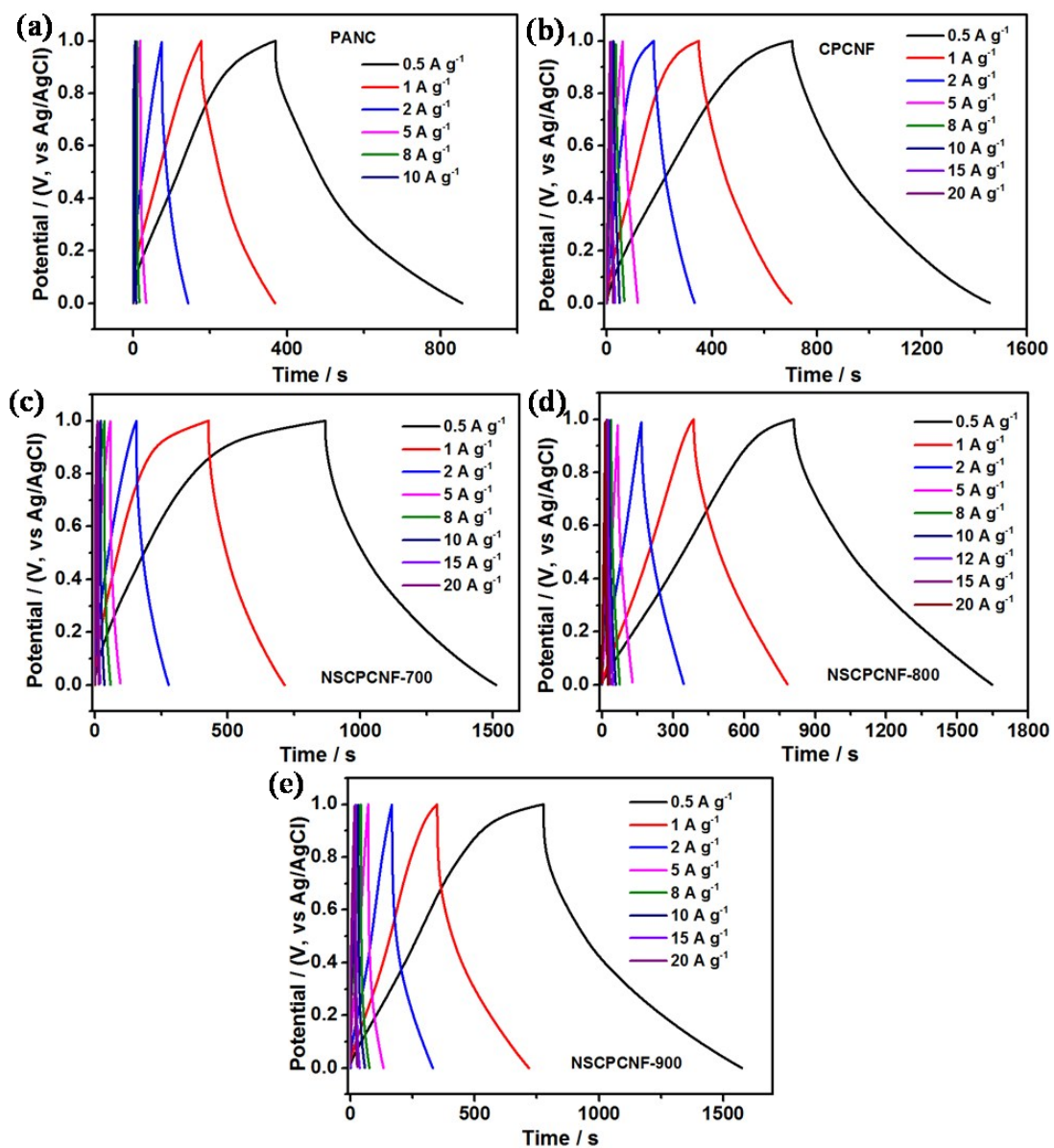


Fig. S11 GCD curves of PANC (a), CPCNF (b), NSCPCNF-700 (c), NSCPCNF-800 (d), NSCPCNF-900 (e) at

different current densities.

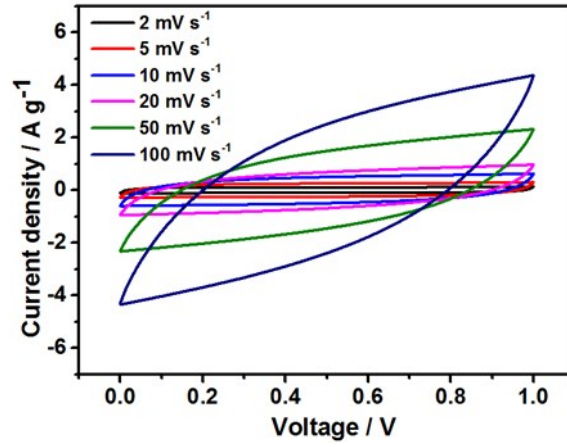


Fig. S12 CV curves of CPCNF//CPCNF at different scan rates.

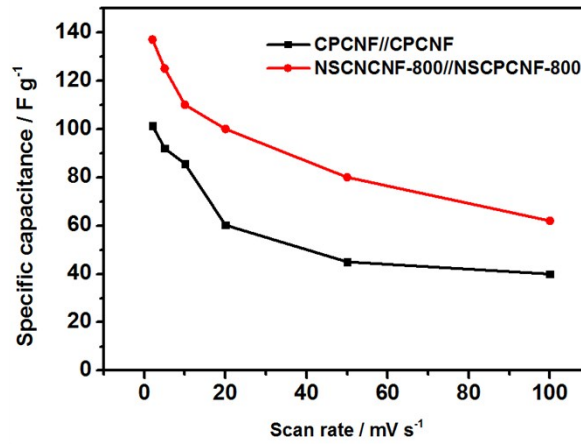


Fig. S13 Specific capacitances of CPCNF//CPCNF and NSCPCNF-800//NSCPCNF-800 at different scan rates.

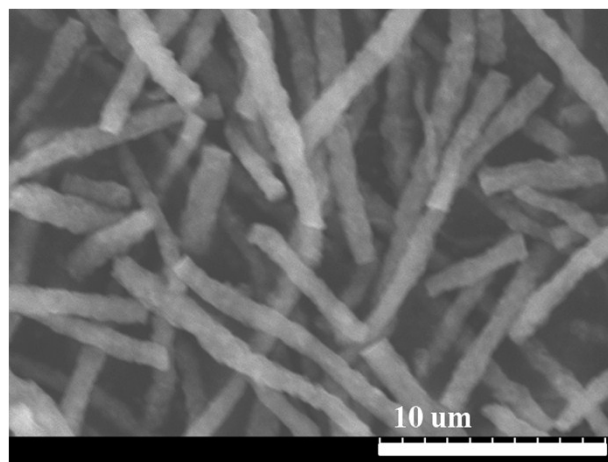


Fig. S14 FESEM image of NSCPCNF-800 after 3000 charge-discharge cycles.

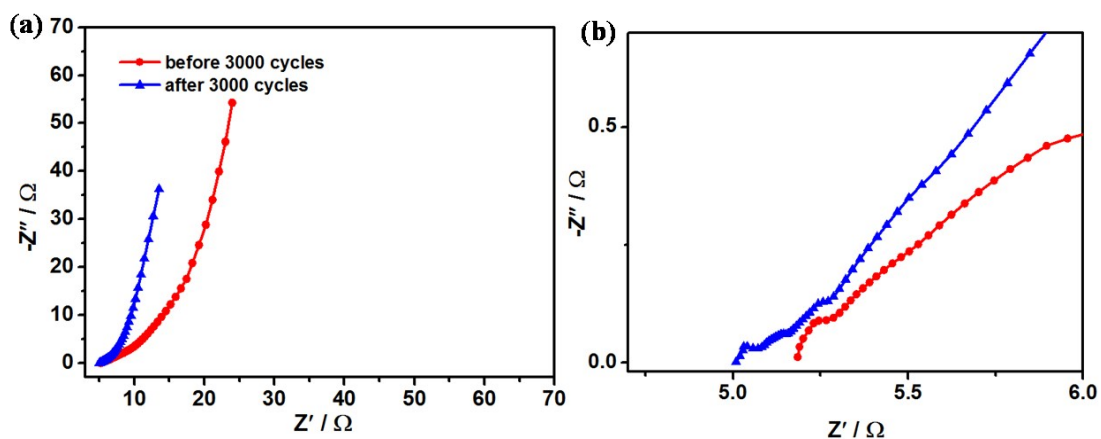


Fig. S15 Nyquist plots (a) and magnified plots in high frequency region (b) of NSCPCNF-800//NSCPCNF-800

before and after 3000 charge-discharge cycles.

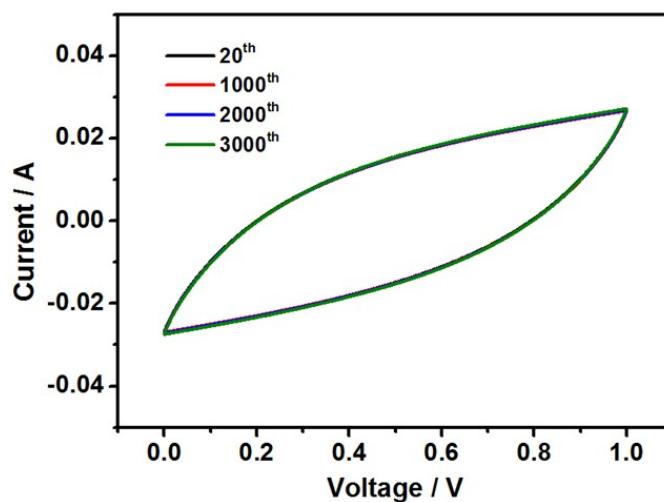


Fig. S16 CV curves of CPCNF//CPCNF in the 20th, 1000th, 2000th and 3000th cycles.

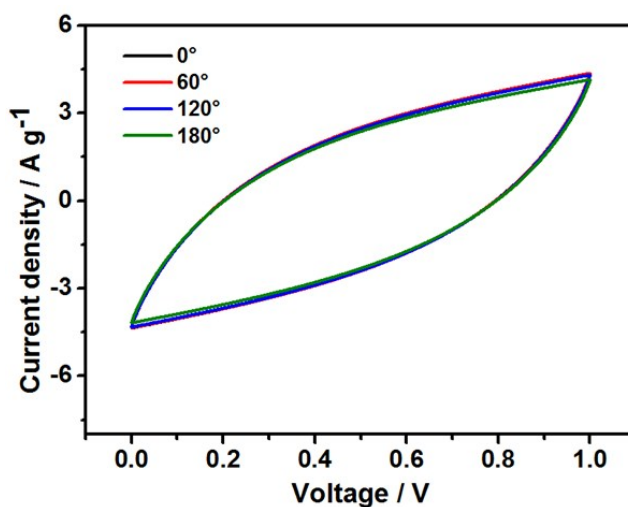


Fig. S17 CV curves of CPCNF//CPCNF at 0°, 60°, 120° and 180° bending angles.

Table S1 Comparison of electrochemical performances of CPCNF and NSCPCNF-800 with the ECNFs

reported in the literatures for supercapacitors.

Electrode material	Current density / A g ⁻¹	Electrolyte	Specific capacitance / F g ⁻¹	Ref.
Hollow particle-based N-doped ECNFs	1	1 mol L ⁻¹ H ₂ SO ₄	307.2	1
N-doped graphitic hierarchically porous ECNFs	0.5	6 mol L ⁻¹ KOH	326	2
N rich hierarchically porous ECNFs	0.5	6 mol L ⁻¹ KOH	302	3
1D hollow ECNFs	1	1 mol L ⁻¹ H ₂ SO ₄	332	4
Micro-/mesoporous ECNFs	1	1 mol L ⁻¹ H ₂ SO ₄	272	5
Mutichannel ECNFs	0.5	6 mol L ⁻¹ KOH	270	6
N rich ECNFs/graphene	0.1	6 mol L ⁻¹ KOH	381	7
N-enriched mesoporous ECNFs	0.2	2 mol L ⁻¹ Li ₂ SO ₄	220	8
Microporous CNFs	0.2	6 mol L ⁻¹ KOH	~ 220	9
Porous ECNFs paper	0.2	6 mol L ⁻¹ KOH	~ 310	10
ECNFs paper	0.05	1 mol L ⁻¹ H ₂ SO ₄	~235	11
Alkali lignin added ECNFs	0.4	6 mol L ⁻¹ KOH	64	12
N, O-doped ECNFs	0.2	6 mol L ⁻¹ KOH	233.1	13

N-doped ECNFs	0.5	1 mol L ⁻¹ H ₂ SO ₄	223.8	14
CPCNF	0.5	1 mol L ⁻¹ H ₂ SO ₄	379	
	1		352	This
NSCPCNF-800	0.5	1 mol L ⁻¹ H ₂ SO ₄	421	work
	1		396	

Table S2 Specific capacitance retentions of NSCPCNF-800//NSCPCNF-800 and CPCNF//CPCNF at different

bending angles.

Bending angle		0°	60°	120°	180°
Specific capacitance retention	NSCPCNF-800//NSCPCNF-800	100%	99.1%	98.8%	97.3%
	CPCNF//CPCNF	100%	99.3%	98.4%	97.6%

References

- 1 L.-F. Chen, Y. Lu, L. Yu and X. W. Lou, *Energy Environ. Sci.*, 2017, **10**, 1777-1783.
- 2 Y. Yao, P. Liu, X. Li, S. Zeng, T. Lan, H. Huang, X. Zeng and J. Zou, *Dalton Trans.*, 2018, **47**, 7316-7326.
- 3 Y. Yao, H. Wu, L. Huang, X. Li, L. Yu, S. Zeng, X. Zeng, J. Yang and J. Zou, *Electrochim. Acta*, 2017, **246**, 606-614.
- 4 C. Wang, C. Liu, J. Li, X. Sun, J. Shen, W. Han and L. Wang, *Chem. Comm.*, 2017, **53**, 1751-1754.

- 5 Y. Li, W. Ou-Yang, X. Xu, M. Wang, S. Hou, T. Lu, Y. Yao and L. Pan, *Electrochim. Acta*, 2018, **271**, 591-598.
- 6 L. Zhang, L. Han, S. Liu, C. Zhang and S. Liu, *RSC Adv.*, 2015, **5**, 107313-107317.
- 7 Q. Xie, S. Zhou, A. Zheng, C. Xie, C. Yin, S. Wu, Y. Zhang and P. Zhao, *Electrochim. Acta*, 2016, **189**, 22-31.
- 8 Q. Liang, L. Ye, Q. Xu, Z.-H. Huang, F. Kang and Q.-H. Yang, *Carbon*, 2015, **94**, 342-348.
- 9 T. Le, Y. Yang, Z. Huang and F. Kang, *J. Power Sources*, 2015, **278**, 683-692.
- 10 C. Ma, Y. Li, J. Shi, Y. Song and L. Liu, *Chem. Eng. J.*, 2014, **249**, 216-225.
- 11 E. J. Ra, E. Raymundo-Piñero, Y. H. Lee and F. Béguin, *Carbon*, 2009, **47**, 2984-2992.
- 12 C. L. Lai, Z. P. Zhou, L. F. Zhang, X. X. Wang, Q. X. Zhou, Y. Zhao, Y. C. Wang, X. F. Wu, Z. T. Zhu and H. Fong, *J. Power Sources*, 2014, **247**, 134-141.
- 13 Q. Li, W. H. Xie, D. Q. Liu, Q. Wang and D. Y. He, *Electrochim. Acta*, 2016, **222**, 1445-1454.
- 14 Y. L. Cheng, L. Huang, X. Xiao, B. Yao, L. Y. Yuan, T. Q. Li, Z. M. Hu, B. Wang, J. Wan and J. Zhou, *Nano Energy*, 2015, **15**, 66-74.